to measure potential-dependent changes in conductivity allows such measurements to be made rapidly in potential regimes where the polymers may have very limited durability.

Acknowledgment. We thank the Office of Naval Research, the Defense Advanced Research Projects Agency, and the National Science Foundation through the M.I.T. Materials Research Laboratory for partial support of this research. We thank Professor Robert J. Silbey for several valuable discussions and we thank Dr. Timothy M. Miller for providing us with 3-phenylthiophene, Professor Stephen L. Buchwald for providing us with 3,4-dimethylpyrrole, and Dr. Ching-Fong Shu for providing us with 1-methyl-1′-(3-(thiophene-3-yl)propyl)-4,4′-bipyridinium·$2PF_6^-$.

The Use of an Electrogenerated Cobalt(I) Porphyrin for the Homogeneous Catalytic Reduction of Dioxygen in Dimethylformamide. Reactions of $[(TMpyP)Co^{II}]^{4+}$ and $[(TMpyP)Co^{I}]^{3+}$ Where TMpyP = *meso*-Tetrakis(1-methylpyridinium-4-yl)porphyrin

D. Sazou, C. Araullo-McAdams, B. C. Han, M. M. Franzen, and K. M. Kadish*

Contribution from the Department of Chemistry, University of Houston, Houston, Texas 77204-5641. *Received April 24, 1990*

Abstract: The one-electron catalytic reduction of dioxygen by electrogenerated *meso*-tetrakis(1-methylpyridinium-4-yl)-porphinatocobalt(I), $[(TMpyP)Co^{I}]^{3+}$, was investigated by cyclic voltammetry, controlled potential coulometry, rotating ring-disk voltammetry, ESR, and UV–visible spectroelectrochemistry. The first reduction of $[(TMpyP)Co^{II}]^{4+}$ in DMF containing 0.1 M tetrabutylammonium perchlorate occurs at $E_{1/2} = -0.49$ V and leads to the formation of $[(TMpyP)Co^{I}]^{3+}$. This cobalt(I) complex is stable under an N_2 atmosphere but in the presence of dissolved O_2 is converted to $[(TMpyP)Co^{II}(O_2^-)]^{3+}$, which is also stable at all potentials up to the reduction of free O_2 (i.e., about −0.80 to −0.90 V vs SCE). A catalytic reduction of dioxygen occurs at $E_p = -0.50$ V by cyclic voltammetry (scan rate = 0.1 V s^{-1}) in DMF solutions containing $[(TMpyP)Co^{II}]^{4+}$ and benzoic anhydride under O_2. The homogeneous reactions of $[(TMpyP)Co^{II}]^{4+}$ and electrogenerated $[(TMpyP)Co^{I}]^{3+}$ with O_2 or O_2^- were characterized and monitored by ESR and UV–visible spectroscopic techniques. A high oxidation state cobalt complex was spectrally characterized during reduction of $[(TMpyP)Co^{II}]^{4+}$ in DMF solutions containing O_2 and benzoic anhydride, while the addition of cyclohexene to this mixture led to the generation of cyclohexene oxide. Integration of the current time curves for reduction of $[(TMpyP)Co^{II}]^{4+}$ in DMF containing benzoic anhydride under O_2 gave a turnover number of ~15 during the first 15 min of bulk electrolysis. The calculated number of turnovers for the conversion of cyclohexene to cyclohexene oxide was 55 during 4.5 h of electrolysis and suggests that the investigated cobalt porphyrin is an extremely efficient catalyst for the reduction of O_2 or the electrocatalytic epoxidation of alkenes.

Introduction

Numerous complexes of water soluble iron(II),[1-6] cobalt(II),[7-12] and manganese(II)[13] porphyrins have been used as catalysts for the multielectron reduction of dioxygen. This reaction can proceed via two electrons to yield hydrogen peroxide or four electrons to give water as the final product in aqueous solutions.

Examples for the electrocatalytic reduction of oxygen by metalloporphyrins are extensive, but very little work has been carried out in nonaqueous organic solvents where the one-electron reduction of free O_2 will generate superoxide anion.[14,15] In fact, only a few examples for the catalytic reduction of O_2 by metalloporphyrins in nonaqueous media have been published.[16-18] These studies utilized a Mn(II) porphyrin as the catalyst which, during the reaction, was converted to an intermediate high oxidation state Mn(V) species[16,17] or to a mixed-valent dimeric manganese Mn(III)/Mn(IV) complex.[18]

The majority of studies involving catalytic reduction of O_2 by cobalt porphyrins have utilized cobalt(II) complexes as catalysts for the heterogeneous reduction of dioxygen to hydrogen peroxide[19,20] or water[21] in aqueous media. This present study also

(1) Ozer, D.; Harth, R.; Mor, U.; Bettelheim, A. *J.Electroanal. Chem.* **1989**, *266*, 109.
(2) Kuwana, T.; Fujihira, M.; Sunakawa, K.; Osa, T. *J. Electroanal. Chem.* **1978**, *88*, 299.
(3) Bettelheim, A.; Kuwana, T. *Anal. Chem.* **1979**, *51*, 2257.
(4) Forshey, P. A.; Kuwana, T. *Inorg. Chem.* **1981**, *80*, 693.
(5) Shigehara, K.; Anson, F. C. *J. Phys. Chem.* **1982**, *86*, 2776.
(6) Bettelheim, A.; Chan, R. J. H.; Kuwana, T. *J. Electroanal. Chem.* **1980**, *110*, 93.
(7) Bettelheim, A.; Chan, R. J. H.; Kuwana, T. *J. Electroanal. Chem.* **1979**, *99*, 391.
(8) Haase, J. *Z. Naturforsch., A* **1968**, *23*, 1000.
(9) Forshey, P. A.; Kuwana, T.; Kobayashi, N.; Osa, T. *Adv. Chem. Ser.* **1982**, *201*, 601.
(10) Durand, R. R., Jr. Ph. D. Thesis, California Institute of Technology, 1984.
(11) Ozer, D.; Parash, R.; Broitman, F.; Mor, U.; Bettelheim, A. *J. Chem. Soc., Faraday Trans. 1* **1984**, *80*, 1139.
(12) Ni, C.-L.; Anson, F. C. *Inorg. Chem.* **1985**, *24*, 4754.
(13) Bettelheim, A.; Ozer, D.; Parash, R. *J. Chem. Soc., Faraday Trans. 1* **1983**, *79*, 1555.
(14) Maricle, D. L.; Hodgson, W. G. *Anal. Chem.* **1965**, *37*, 1562.
(15) Sawyer, D. T.; Roberts, J. L., Jr. *J. Electroanal. Chem.* **1966**, *12*, 90.
(16) Creager, S. E.; Raybuck, S. A.; Murray, R. W. *J. Am. Chem. Soc.* **1986**, *108*, 4225.
(17) Creager, S. E.; Murray, R. W. *Inorg. Chem.* **1987**, *26*, 2612.
(18) Perrée-Fauvet, M.; Gaudemer, A.; Bonvoisin, J.; Girerd, J. J.; Boucly-Goester, C.; Boucly, P. *Inorg. Chem.* **1989**, *28*, 3533.
(19) Durand, R. R.; Anson, F. C. *J. Electroanal. Chem.* **1982**, *134*, 273.
(20) Chan, R. J. H.; Su, Y. O.; Kuwana, T. *Inorg. Chem.* **1985**, *24*, 3777.

0002-7863/90/1512-7879$02.50/0

explores the use of a cobalt porphyrin for the catalytic reduction of O_2 but differs from the previous published work in that cobalt(I) rather than cobalt(II) is the reactive species which participates in the reduction. The investigated catalyst is electrogenerated *meso*-tetrakis(1-methylpyridinium-4-yl)porphinatocobalt(I), $[(TMpyP)Co^{I}]^{3+}$. $[(TMpyP)Co^{II}]^{4+}$ has previously been used as a catalyst for the electrocatalytic reduction of dioxygen in aqueous media,[7-12,20] but this reaction does not occur for the Co(II) derivative in nonaqueous media.

Experimental Section

Instrumentation. Cyclic voltammetry, rotating disc voltammetry, and controlled potential coulometry were performed with the use of a conventional three-electrode cell. A 0.032 cm^2 gold-button or a 0.19 cm^2 glassy carbon disk served as the working electrode for cyclic voltammetry. A platinum wire was utilized as the counter electrode. The reference electrode was a homemade saturated calomel electrode (SCE) which was separated from the bulk solution by a glass frit. All potentials are referenced to the SCE.

The rotating ring-disk assembly (RRDE, Pine Instrument Co.) consisted of a 0.19 cm^2 glassy carbon disk surrounded by a platinum ring. The surfaces of both electrodes were polished with alumina powder and then washed with dilute H_2SO_4, followed by doubly distilled water. An electrochemical pretreatment of the electrodes in deoxygenated 0.1 M KCl was then carried out. This involved cycling the potential of the disk between −0.6 and +0.2 V and that of the ring between 0.0 and +1.0 V until minimum residual currents were obtained.

An IBM Model EC 225 voltammetric analyzer was used for cyclic voltammetric measurements and a double potentiostat (RDE-4, Pine Instrument Co.) was used for rotating ring-disk measurements. This latter instrument was coupled with a Hewlett-Packard 709A measurement plotting system and an MSR high-performance rotator (Pine Instrument Co.). An EG&G PAR Model 173 potentiostat/galvanostat coupled with a Houston Instrument 2000 X-Y recorder was utilized to perform bulk controlled potential electrolysis. A large platinum gauze electrode was used as the working electrode in these experiments.

Thin-layer spectroelectrochemical measurements were carried out with an IBM Model EC 225 voltammetric analyzer and a Model 6500 Tracor Northern Rapid Scan spectrometer which was coupled to an IBM PC-XT computer. The thin-layer cell utilized a gold-gauze working electrode and had a design similar to a Pt thin-layer cell described in the literature.[22] UV-visible data were also obtained with an IBM Model 9430 spectrophotometer.

ESR spectra were recorded with an IBM Model ER 100D spectrometer. The g values were calculated with respect to diphenylpicrylhydrazide (DPPH) which has a signal at $g = 2.0036 \pm 0.0003$. Low temperatures were obtained by using a stream of nitrogen which had been passed through a heat exchanger immersed in liquid nitrogen.

Gas chromatograms were obtained with a Hewlett-Packard Model 5890A gas chromatograph coupled with a Hewlett-Packard Model 3392 integrator. Aliquots of DMF solutions containing $[(TMpyP)Co^{II}]^{4+}$, TBAP, benzoic anhydride, and O_2 were removed prior to and during bulk controlled potential electrolysis of the porphyrin and analyzed by gas chromatography. Nitrogen was used as the carrier gas with FID detection. The column used for analyses was a 10-ft packed column with 10% TCEP (1,2,3-tris-(2-cyanoethoxy)propane) on 100/120 chromosorb. The column temperature was initially set at 60 °C and was increased at a rate of 5 °C/min until a final temperature of 120 °C was reached. This temperature was then held for 28 min. The experimentally determined retention times under these conditions were as follows: cyclohexene, 1.7 min; cyclohexene oxide, 10.7 min; DMF, 33.5 min.

The partial pressure of O_2 was varied by using a Matheson Dyna-Blender Model 8250 flowmeter.

Chemicals. $[(TMpyP)Co^{II}]^{4+}$ was synthesized as the Cl^- salt by using literature methods.[23] Tetra-*n*-butylammonium perchlorate (TBAP) was purchased from Fluka Chemicals G.R. The salt was twice recrystallized from absolute ethyl alcohol and dried in a vacuum oven at 40 °C for at least 1 week prior to use. Dimethylformamide (DMF), purchased from J. T. Baker, was distilled twice under vacuum over 4Å molecular sieves prior to use. Benzoic anhydride was purchased from Aldrich and used as received. Oxygen was obtained from Big Three Ind. and was of high purity (99.995%, min). Cyclohexene was obtained from Mallinckrodt, while cyclohexene oxide was obtained from Aldrich. Both samples were used without further purification.

Solutions of superoxide ion were prepared by dissolving powdered KO_2 (Aldrich) and *cis*-dicyclohexano-18-crown-6 (Aldrich) in dry DMF as described in the literature.[24]

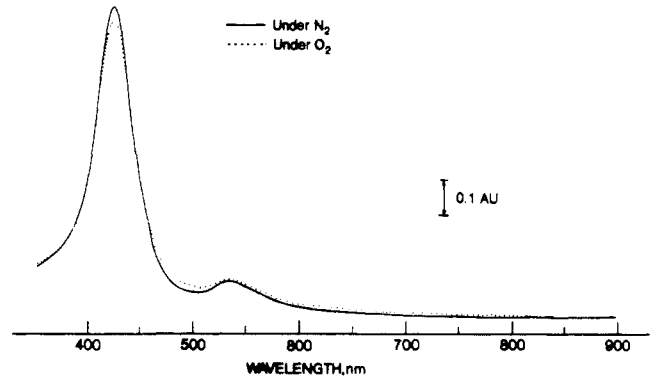

Figure 1. UV-visible spectrum of $[(TMpyP)Co^{II}]^{4+}$ in DMF, 0.1 M TBAP under N_2 (—) and under O_2 (···).

Results and Discussion

Spectral Characterization of $[(TMpyP)Co^{II}]^{4+}$ under O_2. Cobalt porphyrins are known to bind O_2 in nonaqueous media and may exist as either a Co(II)–O_2 or a Co(III)–O_2^- complex depending upon the nature of the porphyrin macrocycle and the exact solution conditions.[19,25-29] $[(TMpyP)Co^{II}]^{4+}$ is also known to bind O_2 in frozen aqueous media.[30] It was therefore necessary to determine if the formation of $[(TMpyP)Co^{II}O_2]^{4+}$ or $[(TMpyP)Co^{III}(O_2^-)]^{4+}$ might also occur in DMF containing 0.1 M TBAP. This was investigated by UV-visible and ESR spectroscopic techniques at both room and low temperature.

The UV-visible spectrum of $[(TMpyP)Co^{II}]^{4+}$ in DMF under an N_2 atmosphere is shown by the solid line in Figure 1. The maximum wavelengths of the complex are located at 426 (Soret) and 534 nm, and these values may be compared to maximum wavelengths of 440 (Soret) and 542 nm in pyridine or 433 (Soret) and 545 nm in dimethyl sulfoxide.[31] The axial binding of a solvent molecule to Co(II) will shift λ_{max} toward higher wavelengths, and the spectrum in Figure 1 of $[(TMpyP)Co^{II}]^{4+}$ in DMF containing 0.1 M TBAP at room temperature under N_2 is consistent with the lack of axially ligated DMF.

Similar UV-visible spectra are obtained for $[(TMpyP)Co^{II}]^{4+}$ in DMF under N_2 or under O_2. There is no significant change in the UV-visible spectrum of the complex at any O_2 concentrations up to 1 atm (see dashed line, Figure 1), nor is there any significant change in the spectrum when the temperature is lowered to −60 °C. This UV-visible data would seem to suggest that $[(TMpyP)Co^{II}O_2]^{4+}$ is not formed (or is formed in only a small quantity) at room temperature. The data also suggest that the oxygen-bound complex is not formed at any temperatures as low as −60 °C in DMF since this type of species would have a UV-visible spectrum characteristic of $Co^{III}O_2^-$.[28] On the other hand, the ESR data clearly show the formation of $[(TMpyP)Co^{II}O_2]^{4+}$ at temperatures below −100 °C. This is shown in Figure 2 which

(21) (a) Collman, J. P.; Marrocco, M.; Denisevich, P.; Koval, C.; Anson, F. C. *J. Electroanal. Chem.* **1979**, *101*, 117. (b) Collman, J. P.; Denisevich, P.; Konai, Y.; Marrocco, M.; Koval, C.; Anson, F. C. *J. Am. Chem. Soc.* **1980**, *103*, 6027.
(22) Lin, X. Q.; Kadish, K. M. *Anal. Chem.* **1985**, *57*, 1498.
(23) Pasternack, R. F.; Francesconi, L.; Raff, D.; Spiro, E. *Inorg. Chem.* **1973**, *12*, 2606.
(24) (a) Ozawa, T.; Hanaki, A. *Inorg. Chim. Acta* **1983**, *80*, 33. (b) Valentine, J. S.; Curtis, A. B. *J. Am. Chem. Soc.* **1975**, *97*, 224.
(25) James, B. R. *The* Porphyrins; Dolphin, D., Ed.; Academic: New York, 1979; Vol. V, p 205.
(26) (a) Walker, F. A. *J. Am. Chem. Soc.* **1970**, *92*, 4235. (b) Walker, F. A. *J. Am. Chem. Soc.* **1973**, *95*, 1154.
(27) (a) Walker, F. A. *J. Magn. Reson.* **1974**, *15*, 201. (b) Walker, F. A.; Beroiz, D.; Kadish, K. M. *J. Am. Chem. Soc.* **1976**, *98*, 3484. (c) Henrici-Olivé, G.; Olivé, S. *Angew. Chem., Int. Ed. Engl.* **1974**, *13*, 29.
(28) Wayland, B. B.; Minkiewicz, J. V.; Abd-Elmageed, M. E. *J. Am. Chem. Soc.* **1974**, *96*, 2795.
(29) (a) Lin, W. C.; Lau, P. W. *J. Am. Chem. Soc.* **1976**, *98*, 1447. (b) Subramanian, J. *Porphyrins and Metalloporphyrins*; Smith, K. M., Ed.; Elsevier: New York, 1975; Chapter 13.
(30) Evans, D. F.; Wood, D. *J. Chem. Soc., Dalton Trans.* **1987**, 3099.
(31) Araullo-McAdams, C.; Kadish, K. M. *Inorg. Chem.* **1990**, *29*, 2749.

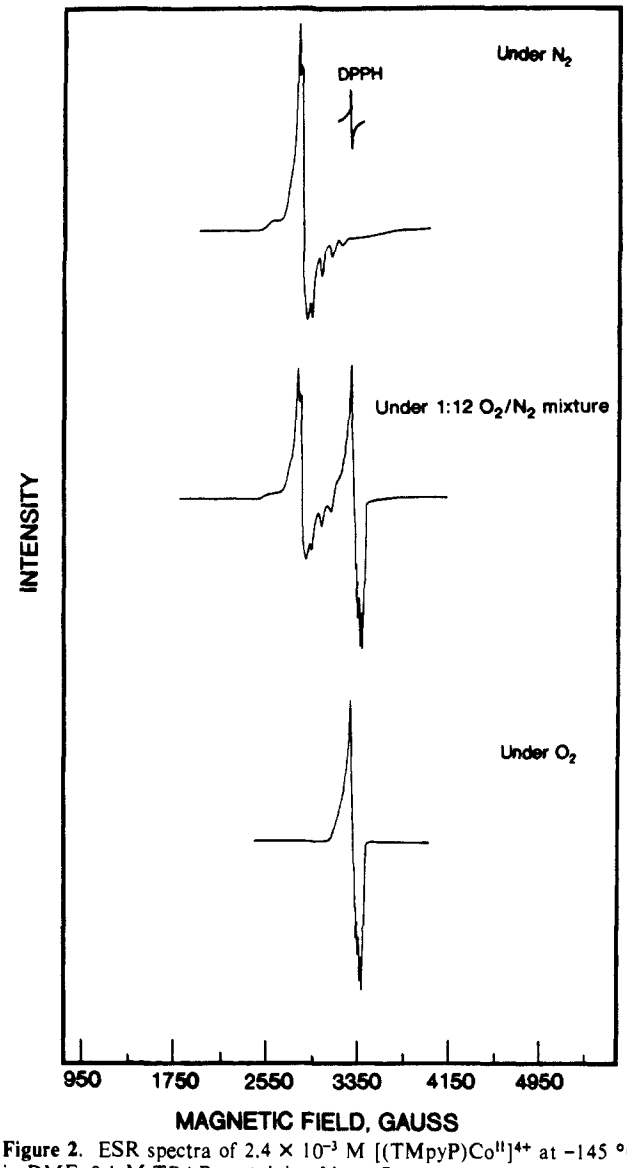

Figure 2. ESR spectra of 2.4×10^{-3} M $[(TMpyP)Co^{II}]^{4+}$ at −145 °C in DMF, 0.1 M TBAP containing N_2 or O_2.

illustrates the ESR spectra at −145 °C for $[(TMpyP)Co^{II}]^{4+}$ under N_2, under O_2, and under a 1:12 O_2/N_2 mixture.

The ESR spectrum of $[(TMpyP)Co^{II}]^{4+}$ under a N_2-atmosphere at −145 °C is typical of a Co(II) porphyrin[29] and is characterized by $g_\perp = 2.34$, $g_\parallel = 2.06$, and $A_\parallel = 83$G. The ESR spectra of $[(TMpyP)Co^{II}]^{4+}$ under O_2 is also typical of a Co(II) porphyrin oxygen complex[25-29] and is characterized by $g = 2.01$ (see Figure 2). Consequently, these spectra suggest that $[(TMpyP)Co^{II}]^{4+}$ can be converted to $[(TMpyP)Co^{II}O_2]^{4+}$ at low temperatures as shown in eq 1.

$$[(TMpyP)Co^{II}]^{4+} + O_2 \Leftrightarrow [(TMpyP)Co^{II}O_2]^{4+} \quad (1)$$

The equilibrium in reaction 1 will depend upon the partial pressure of O_2 and upon the solution temperature. The ESR signal intensity of $[(TMpyP)Co^{II}]^{4+}$ decreases while that for $[(TMpyP)Co^{II}O_2]^{4+}$ increases with an increase in the partial pressure of O_2. The resulting ESR spectrum at −145 °C under a 1:12 O_2/N_2 gas mixture indicates that an approximate 50% mixture of $[(TMpyP)Co^{II}]^{4+}$ and $[(TMpyP)Co^{II}O_2]^{4+}$ is in solution under these conditions.

The equilibria in reaction 1 was also evaluated by varying the temperature of the solution under a 1:12 O_2/N_2 mixture from −145 °C to 23 °C. As the temperature was increased from −145 °C, the signals due to $[(TMpyP)Co^{II}O_2]^{4+}$ and $[(TMpyP)Co^{II}]^{4+}$ both decreased in intensity and finally disappeared. ESR spectra of Co(II) porphyrins are not observed at room temperature because of short relaxation times. Thus, it is not possible to determine by ESR techniques whether O_2 is still complexed to $[(TMpyP)Co^{II}]^{4+}$ at room temperature. On the other hand, the room-temperature binding constants of O_2 with other cobalt(II) porphyrin complexes are small in nonaqueous media,[25-27] and it is assumed that this is also the case in the present study.

Electrochemistry of $[(TMpyP)Co^{II}]^{4+}$ under O_2. The electroreduction of $[(TMpyP)Co^{II}]^{4+}$ under N_2 occurs in four reversible steps to give $[(TMpyP)Co^{II}]^{2-}$ as the final product.[31] The first reduction involves a one-electron transfer and occurs at $E_{1/2} = -0.49$ V vs SCE. The second reduction also involves a one-electron transfer and occurs at $E_{1/2} = -0.74$ V. The last two processes each involve two electrons and occur at $E_{1/2} = -0.89$ and −0.98 V.

In this present study we have focused only on the first reduction which involves the conversion of $[(TMpyP)Co^{II}]^{4+}$ to $[(TMpyP)Co^{I}]^{3+}$. This reaction is illustrated in Figure 3a which shows cyclic voltammograms and an analysis of the peak current for the reduction of $[(TMpyP)Co^{II}]^{4+}$ in DMF containing 0.1 M TBAP under nitrogen. The peak currents for this reduction increase linearly with the square root of scan rate, ν. The anodic-to-cathodic peak current ratio, i_{pa}/i_{pc}, is close to unity, and the peak-to-peak separation, $|E_{pc} - E_{pa}|$, is equal to 75 ± 5 mV over a potential scan range of 25–300 mV s^{-1}. These data are internally self-consistent and indicate a one-electron diffusion-controlled quasi-reversible process with no kinetic complications.

The reduction of $[(TMpyP)Co^{II}]^{4+}$ in DMF, 0.1 M TBAP under O_2 is irreversible, and the peak potential maximum is shifted anodically from the value under N_2 as shown by the cyclic voltammograms in Figure 3b. However, the shape of the cathodic process, as determined by $|E_p - E_{p/2}|$, remains constant at 75 ± 5 mV (Figure 3b) and suggests an EC-type mechanism involving electrogenerated $[(TMpyP)Co^{I}]^{3+}$. The peak currents for this process are enhanced by about 16% with respect to values for the same reduction under a N_2 atmosphere, but the values of i_p remain proportional to $\nu^{1/2}$. This shows that the electroreduction remains diffusion controlled under an O_2 atmosphere. The half-peak potential, $E_{p/2}$, shifts cathodically by 55 mV per 10-fold increase of potential scan rate and is consistent with a one-electron reduction step followed by a homogeneous irreversible chemical reaction.

A chemical reaction does not occur under N_2 and suggests that the homogeneous reaction involves both $[(TMpyP)Co^{I}]^{3+}$ and dissolved O_2 in solution. As will be later demonstrated, the overall homogeneous reaction initially proceeds via the binding of O_2 to give $[(TMpyP)Co^{II}(O_2^-)]^{3+}$ as shown in reaction 2.

$$[(TMpyP)Co^{I}]^{3+} + O_2 \Leftrightarrow [(TMpyP)Co^{II}(O_2^-)]^{3+} \quad (2)$$

The assignment of a Co(II)–O_2^- adduct[32] rather than a Co(I)–O_2 species as the product in reaction 2 comes from electrochemical and spectroscopic experiments carried out in the presence of benzoic anhydride. Benzoic anhydride is a known O_2^- scavenger,[34] and a catalytic reduction of O_2 should result if $[(TMpyP)Co^{II}(O_2^-)]^{3+}$ is formed as a product of the $[(TMpyP)Co^{II}]^{4+}$ reduction under O_2. This is indeed the case as will be shown in the following discussion.

Cyclic voltammograms for the reduction of $[(TMpyP)Co^{II}]^{4+}$ in DMF containing benzoic anhydride under N_2 are identical with those under N_2 alone (Figure 3a). This indicates that benzoic anhydride does not react with $[(TMpyP)Co^{II}]^{4+}$ or with electrogenerated $[(TMpyP)Co^{I}]^{3+}$. In contrast, the reduction of $[(TMpyP)Co^{II}]^{4+}$ in DMF containing both dioxygen and benzoic anhydride is irreversible and is also characterized by a substantially increased cathodic peak current. This is shown in Figure 3c which illustrates cyclic voltammograms and an analysis of i_p for the first potential scan vs $\nu^{1/2}$.

The cathodic peak current for the reduction of $[(TMpyP)Co^{II}]^{4+}$ diminishes on the second potential scan and this is attributed to a deactivation of the electrode by adsorption of either the final product or a reaction intermediate. However, the reduction currents are well defined on the first scan as shown in Figure 3c. The plot of i_p vs $\nu^{1/2}$ is linear (indicating diffusion control), and the value of $\Delta i_p/\Delta\nu^{1/2}$ is almost 40 times higher than for the

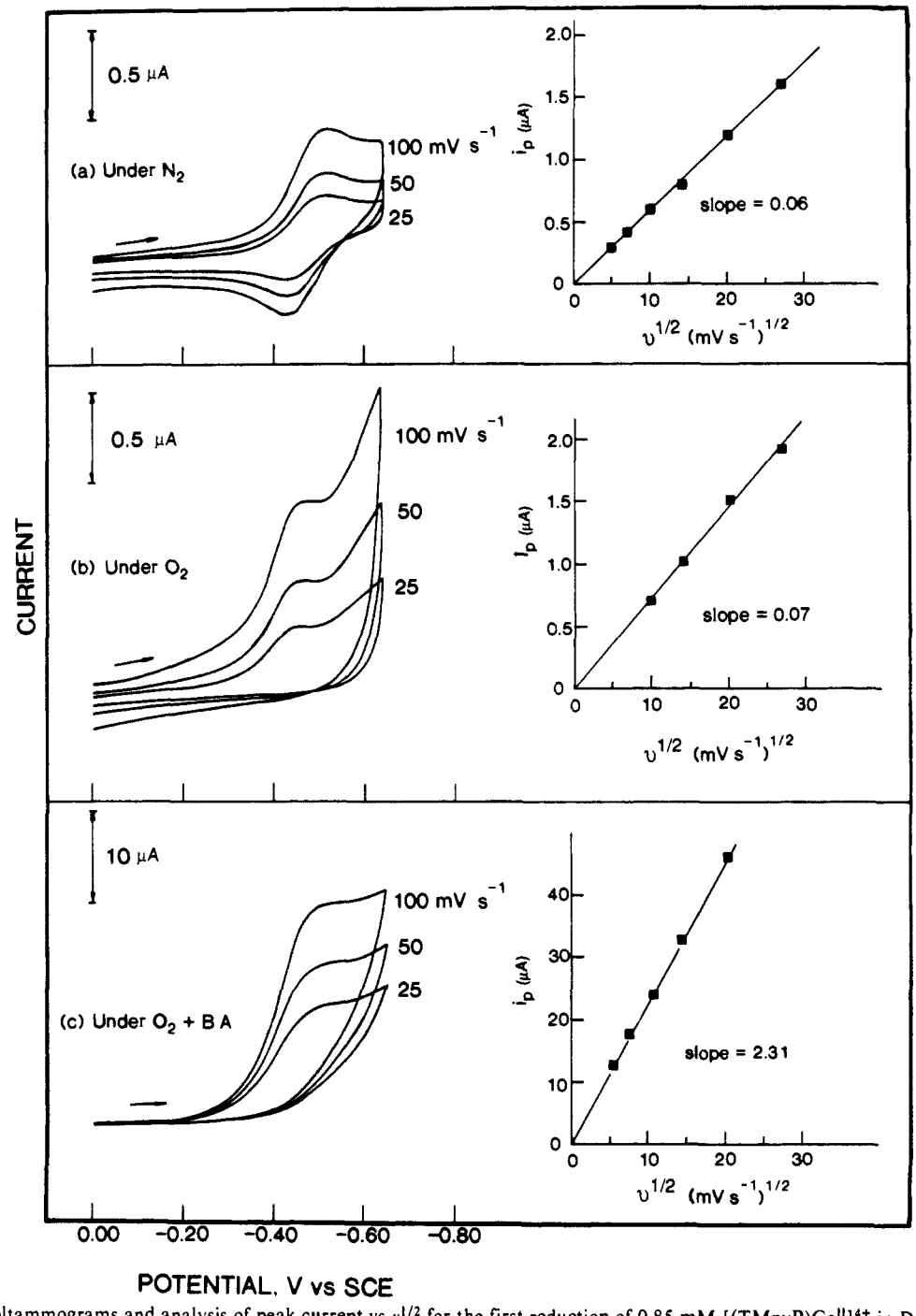

Figure 3. Cyclic voltammograms and analysis of peak current vs $\nu^{1/2}$ for the first reduction of 0.85 mM $[(TMpyP)Co^{II}]^{4+}$ in DMF, 0.1 M TBAP at a gold electrode (a) under N_2, (b) under O_2, and (c) under O_2 in solutions containing 0.1 M benzoic anhydride.

reaction under N_2 (Figure 3a) or under O_2 (Figure 3b) in the absence of benzoic anhydride. These data are thus consistent with the formation of a cobalt(II)–superoxo adduct under O_2 and the electrocatalytic reduction of O_2 to regenerate $[(TMpyP)Co^{II}]^{4+}$ in DMF solutions containing benzoic anhydride.

The simplified sequence of reactions which occur under these conditions is shown in Scheme I which does not indicate the products formed in the reaction between $[(TMpyP)Co^{II}(O_2^-)]^{3+}$ and benzoic anhydride. However, this part of the reaction scheme was investigated in detail, and an expanded overall catalytic mechanism is presented in later sections of the manuscript.

The electrocatalytic reduction of O_2 was also investigated at a glassy carbon electrode in DMF containing different concentrations of O_2[35] and $[(TMpyP)Co^{II}]^{4+}$. Cyclic voltammograms of $[(TMpyP)Co^{II}]^{4+}$ at different concentrations in the presence of O_2 are shown in Figure 4. The electroreduction of free O_2 in DMF occurs at $E_{pc} = -0.90$ V in the absence of $[(TMpyP)Co^{II}]^{4+}$ for a scan rate of 0.1 V s^{-1} (see Figure 4a). This value may be compared to the experimentally measured $E_{pc} = -0.55$ V for the catalytic reduction of O_2 in the presence of $[(TMpyP)Co^{II}]^{4+}$ at the same glassy carbon electrode (scan rate = 0.1 V s^{-1}) or the $E_p = -0.50$ V for the irreversible reduction of $[(TMpyP)Co^{II}]^{4+}$ at a gold electrode (Figure 3c) under the same experimental conditions.

The catalytic reduction current at $E_{pc} = -0.55$ V increases as the concentration of $[(TMpyP)Co^{II}]^{4+}$ is increased from 0.11 to 0.53 mM in DMF solutions containing 2.44 mM O_2. At the same time, the diffusion current for the reduction of free O_2 decreases as shown in Figure 4b. These data clearly indicate that the catalytic reduction at $E_{pc} = -0.55$ V involves O_2 and electrogenerated $[(TMpyP)Co^{I}]^{3+}$ which is formed at similar potentials in DMF solutions (see cyclic voltammograms in Figure 3a). This dioxygen adduct of Co(I) is stable at all potentials up to the reduction of free O_2.

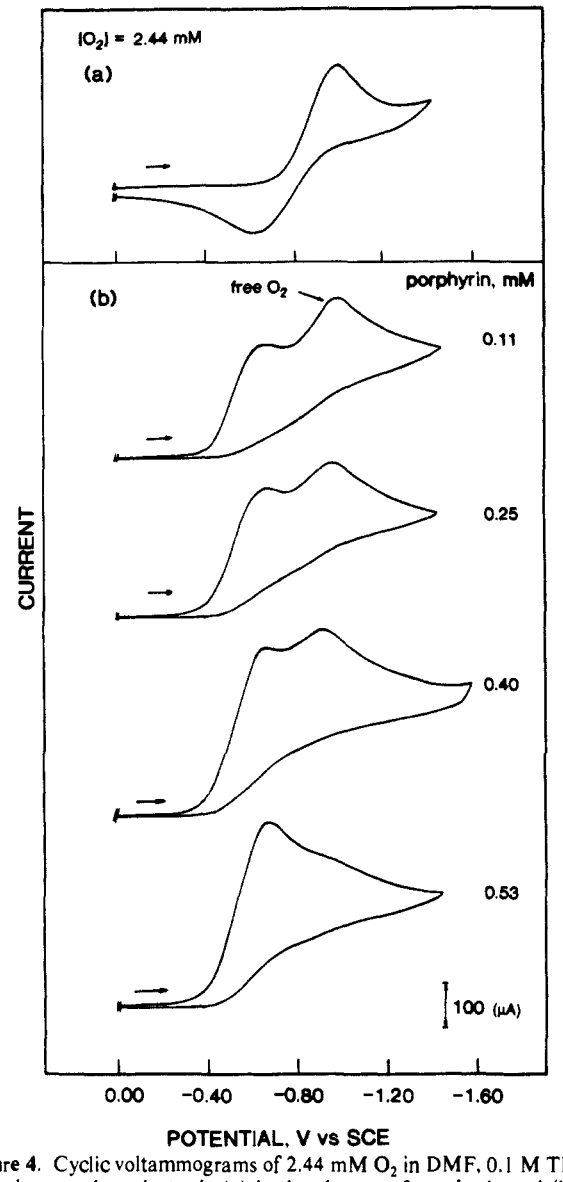

Figure 4. Cyclic voltammograms of 2.44 mM O_2 in DMF, 0.1 M TBAP at a glassy carbon electrode (a) in the absence of porphyrin and (b) in solutions containing 0.1 M benzoic anhydride and 0.11–0.53 mM $[(TMpyP)Co^{II}]^{4+}$. Scan rate = 0.1 V s^{-1}.

Scheme I

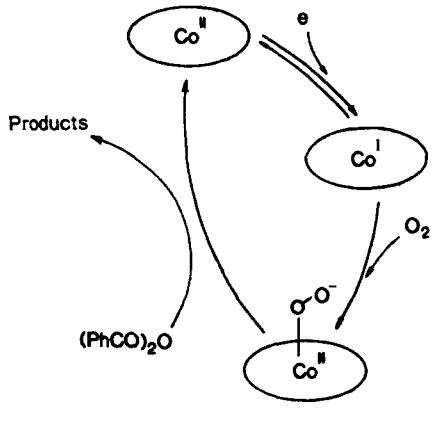

As expected, the catalytic current for O_2 reduction does not change substantially with changes in the concentration of porphyrin in solution but is dependent upon the O_2 concentration. This is shown in Figure 5 for the reduction of 0.25 mM $[(TMpyP)Co^{II}]^{4+}$ in DMF containing 0.1 M TBAP, 0.1 M benzoic anhydride, and various concentrations of O_2. A reduction occurs at E_{pc} = −0.55 V in solutions containing 0.45 mM O_2 and 0.25 mM porphyrin. Only a small peak for the reduction of free O_2 is obtained under these conditions indicating that all of the O_2 in solution is reduced at potentials corresponding to the first reduction of $[(TMpyP)Co^{II}]^{4+}$. The currents for the first reduction increase about 3-fold as the O_2 concentration is increased from 0.45 to 2.44 mM. At the same time, a peak for the reduction of free O_2 (at E_{pc} = −0.90 V) also appears.

The value of i_{pc} for the reduction at E_{pc} = −0.55 V in Figure 5 is not proportional to the porphyrin bulk concentration but rather increases linearly with O_2 concentration as shown in Figure 6.

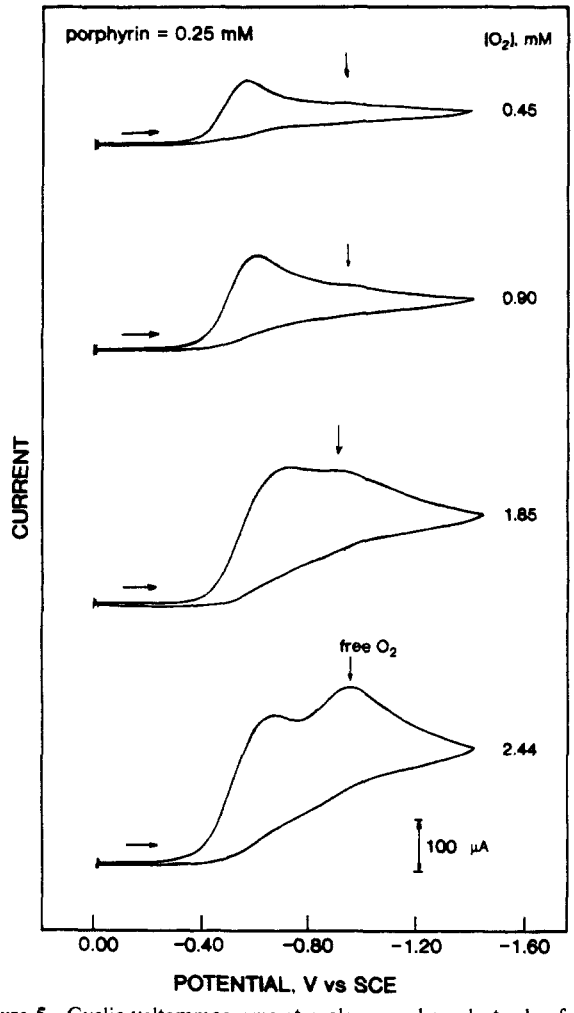

Figure 5. Cyclic voltammograms at a glassy carbon electrode of 0.25 mM $[(TMpyP)Co^{II}]^{4+}$ in DMF, 0.1 M TBAP containing 0.1 M benzoic anhydride and 0.45–2.44 mM O_2. Scan rate = 0.1 V s^{-1}.

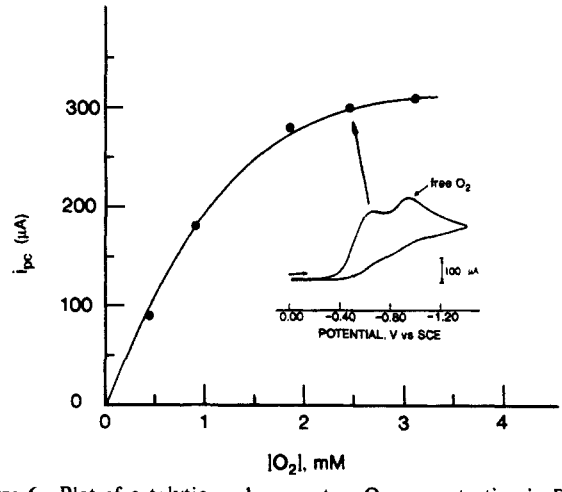

Figure 6. Plot of catalytic peak current vs O_2 concentration in DMF containing 0.25 mM $[(TMpyP)Co^{II}]^{4+}$.

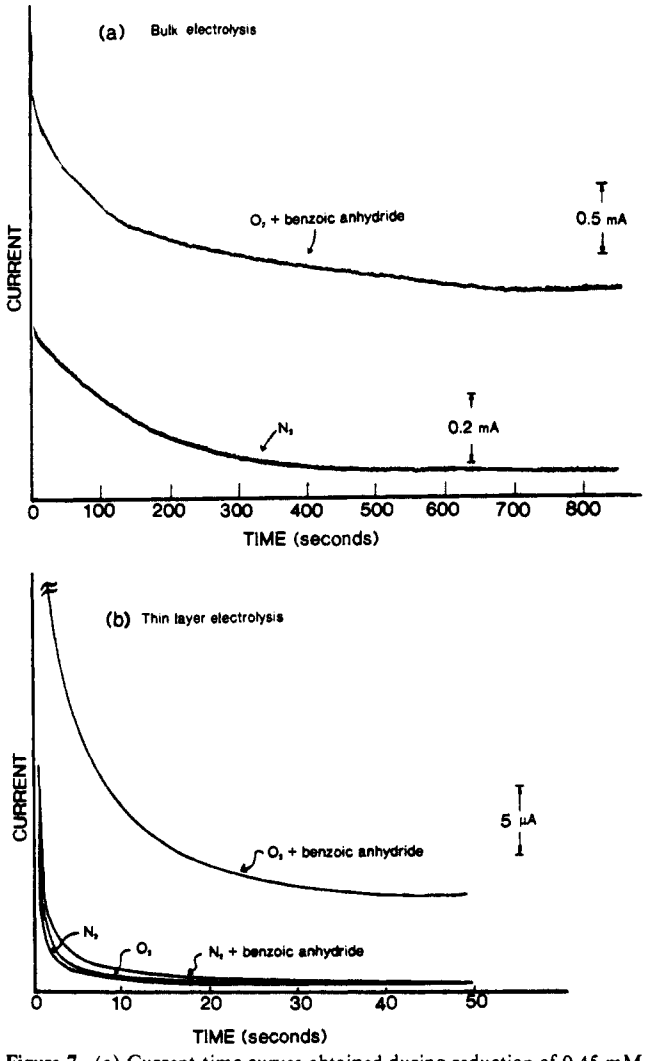

Figure 7. (a) Current-time curves obtained during reduction of 0.45 mM $[(TMpyP)Co^{II}]^{4+}$ at −0.58 V vs SCE (a) by bulk electrolysis and (b) by thin-layer electrolysis.

These data were taken from voltammograms of the type shown in Figure 5 and give further evidence that O_2 is catalytically reduced at about $E_{pc} = -0.55$ V.

Current-time curves obtained during bulk and thin-layer controlled potential electroreduction of 0.45 mM $[(TMpyP)Co^{II}]^{4+}$ under various conditions are shown in Figure 7. The reduction under N_2 gives a global 1.0 ± 0.1 electrons transferred during thin layer and bulk electrolysis at −0.58 V. A steady-state current is quickly reached in both cases, and the current-time curves are consistent with a one-electron transfer. In contrast, the final steady-state current for reduction of $[(TMpyP)Co^{II}]^{4+}$ is significantly higher when both dioxygen and benzoic anhydride are present in the DMF solution. This increase is due to the reaction of $[(TMpyP)Co^{II}(O_2^-)]^{3+}$ with benzoic anhydride which results in a regeneration of initial $[(TMpyP)Co^{II}]^{4+}$. This Co(II) complex is then quickly reduced at −0.58 V to give $[(TMpyP)Co^{I}]^{3+}$ which again binds with molecular oxygen. Integration of the bulk current-time curve in DMF containing benzoic anhydride under O_2 (Figure 7a) gives a turnover number of ~15 during the first 15 min of electrolysis.

The catalytic electroreduction of oxygen was also studied at a rotating ring-disc electrode (RRDE) in order to ascertain the possible formation of peroxide dianion, O_2^{2-}, or hydroxide ion[37]

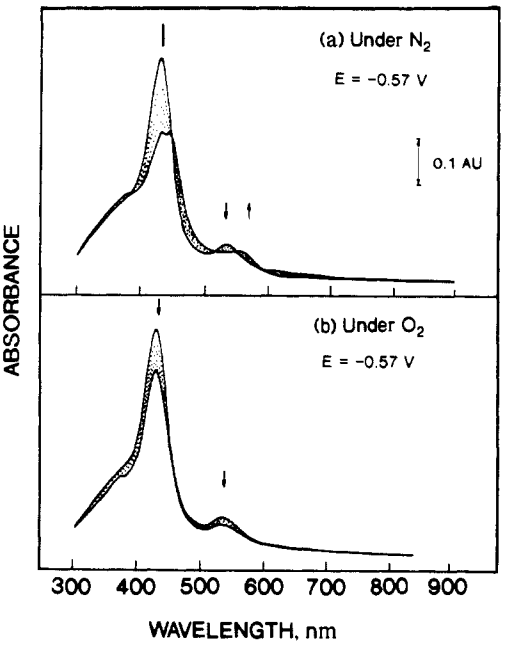

Figure 8. Time-resolved UV–visible spectra recorded during thin-layer electroreduction of $[(TMpyP)Co^{II}]^{4+}$ at −0.57 V in DMF, 0.2 M TBAP (a) under N_2 and (b) under O_2.

as a final product in the electroreduction. The glassy carbon disc potential was scanned from 0.00 to −1.00 V at a scan rate of 25 mV s^{-1}, while the potential of the Pt ring electrode was maintained at 0.80 V. The resulting RRDE voltammograms for reduction of $[(TMpyP)Co^{II}]^{4+}$ containing various O_2 concentrations in the absence and presence of benzoic anhydride show that the ring current is negligible under the given experimental conditions. This suggests that neither free O_2^{2-} nor free OH^- are formed during the electrocatalytic reduction of O_2 since both of these two-electron reduction products from O_2 would be oxidized at about 0.80 V.

Spectroelectrochemistry of $[(TMpyP)Co^{II}]^{4+}$ under N_2 or O_2. The electrocatalytic reduction of O_2 by $[(TMpyP)Co^{I}]^{3+}$ was spectroscopically monitored during thin-layer electrolysis at a gold optically transparent electrode. Time-resolved spectra obtained during controlled potential reduction of $[(TMpyP)Co^{II}]^{4+}$ under N_2 are shown in Figure 8a. The final spectrum has absorptions at 431, 441, and 550 nm and is consistent with the formation of $[(TMpyP)Co^{I}]^{3+}$ as a final stable product in the reduction. A similar Co(I) spectrum was obtained after controlled potential reduction of $[(TMpyP)Co^{II}]^{4+}$ in Me_2SO.[31] The spectral changes in Figure 8a are reversible, and the spectrum of the original $[(TMpyP)Co^{II}]^{4+}$ complex could be obtained by setting the applied potential to 0.00 V after complete electroreduction. Spectral changes similar to those in Figure 8a were also obtained under N_2 in the presence of benzoic anhydride. This result is consistent with the electrochemical data which show the absence of a chemical reaction between benzoic anhydride and the electrogenerated $[(TMpyP)Co^{I}]^{3+}$.

Spectral changes obtained during electrolysis of $[(TMpyP)Co^{II}]^{4+}$ in DMF under O_2 are shown in Figure 8b. The final spectrum generated under these experimental conditions has bands at 426 and 533 nm and is attributed to electrogenerated $[(TMpyP)Co^{II}(O_2^-)]^{3+}$. These changes are irreversible, and no changes in the spectra resulted when the applied potential was reset to 0.00 V. The absorption bands of $[(TMpyP)Co^{II}(O_2^-)]^{3+}$ are similar to those of $[(TMpyP)Co^{II}]^{4+}$ but less intense.

Controlled potential reduction of $[(TMpyP)Co^{II}]^{4+}$ at a Au electrode in O_2 saturated DMF solutions containing 0.2 M TBAP

(32) An alternate assignment of the dioxygen species as $[(TMpyP)Co^{III}(O_2^{2-})]^{3+}$ is also possible in light of recent results which shows that (OEP)Fe and O_2^- react to give $[(OEP)Fe^{III}(O_2^{2-})]^-$ as a stable product.[33] However, as demonstrated in this present paper, the UV–visible spectrum of $[(TMpyP)Co(O_2)]^{3+}$ closely resembles a Co(II) porphyrin complex rather than a Co(III) species.

(33) Burstyn, J. N.; Roe, J. A.; Miksztal, A. R.; Shaevitz, B. A.; Lang, G.; Valentine, J. S. *J. Am. Chem. Soc.* **1988**, *110*, 1382.
(34) Khenkin, A. M.; Shteinman, A. A. *Oxid. Commun.* **1983**, *4*, 443.
(35) The concentration of O_2 in different DMF solutions was determined by assuming a maximum solubility of 3.1 mM in DMF.[36]
(36) James, H. J.; Broman, R. F. *Anal. Chim. Acta* **1969**, *48*, 411.
(37) Goolsby, A. D.; Sawyer, D. T., *Anal. Chem.* **1967**, *39*, 411.

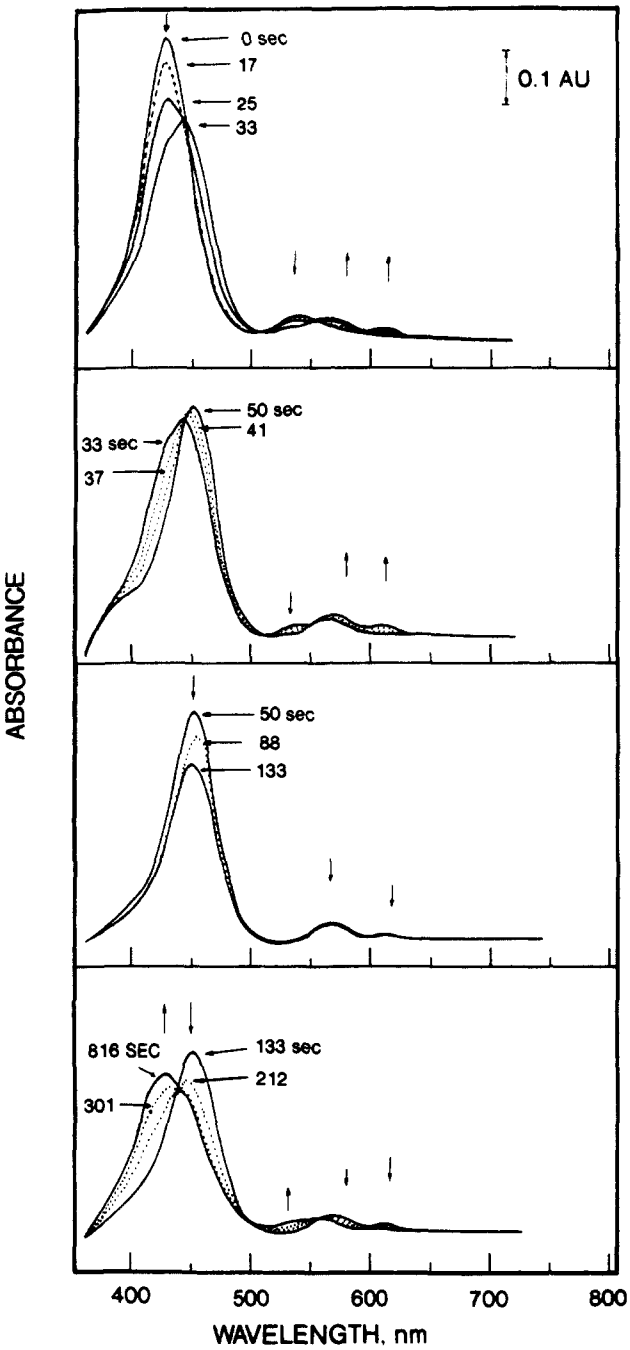

Figure 9. Time-resolved UV-visible spectra recorded during thin-layer electroreduction of $[(TMpyP)Co^{II}]^{4+}$ at −0.57 V in an O_2 saturated solution of DMF containing 0.1 M benzoic anhydride and 0.2 M TBAP.

and 0.1 M benzoic anhydride gives the time-resolved thin-layer spectra shown in Figure 9. Similar spectral changes were obtained at a Pt thin-layer electrode, but the exact times for generation of a specific spectrum varied slightly.

Several different cobalt porphyrin species are spectrally detectable in Figure 9. These are the initial Co(II) porphyrin, a reduced Co(I) porphyrin with bound O_2, at least one high oxidation state complex of the cobalt porphyrin, and a final Co(II) or Co(I) species after the cycle is complete. The spectral changes can also be broken down into several discrete stages. The first stage occurs during the first 17 s of electrolysis as the initial $[(TMpyP)Co^{II}]^{4+}$ complex is converted to a species with a spectrum similar to that of $[(TMpyP)Co^{II}(O_2^-)]^{3+}$ (see Figure 8b).

The second stage occurs between 17 and 50 s and gives a transient species with absorption maxima at 445 and 559 nm. This spectrum is shown at 33 s in Figure 9 and is similar to that of $[(TMpyP)Co^{III}]^{5+}$ which has absorptions at 445 and 554 nm in DMF under N_2. This high oxidation state species is in equilibrium

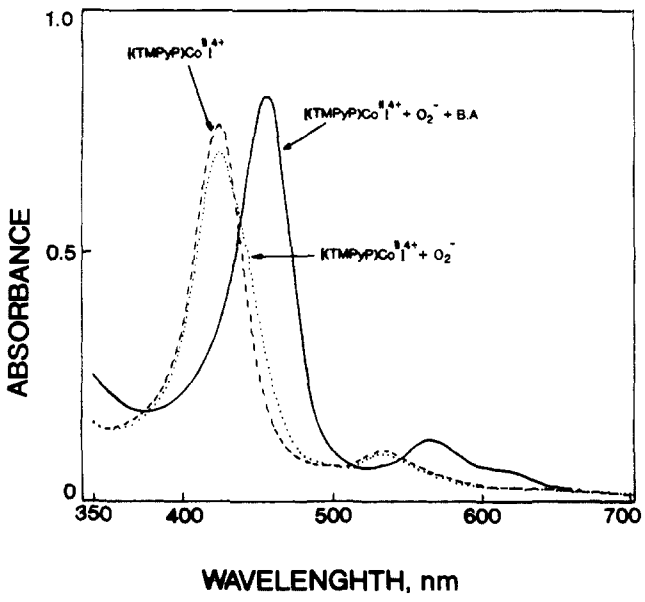

Figure 10. UV-visible spectra of $[(TMpyP)Co^{II}]^{4+}$ in DMF, 0.2 M TBAP under nitrogen (––), under nitrogen in the presence of O_2^- (···), and under nitrogen in the presence of O_2^- and benzoic anhydride (—).

Scheme II

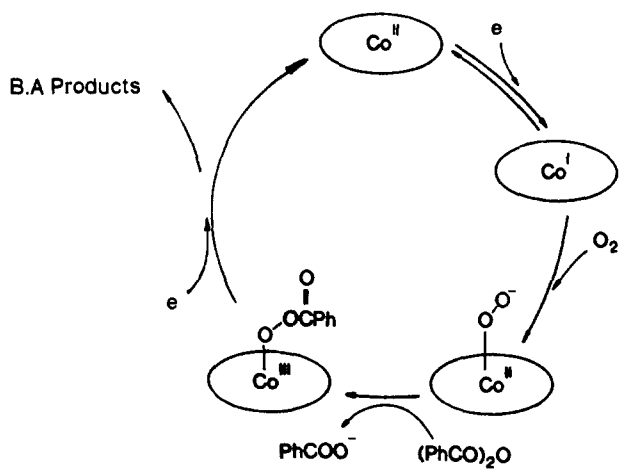

with $[(TMpyP)Co^{II}(O_2^-)]^{3+}$ as demonstrated by the isosbestic point at 442 nm. The third stage occurs between 50 and 175 s of electrolysis in Figure 9 and gives a spectrum with absorption maxima at 451 and 566 nm. The shape of this spectrum does not change from 50 to 175 s, but the intensity of the bands continuously decrease indicating the consumption of this species. Final changes in the UV–vis spectra occur between 175 and 900 s and lead to a species with bands at 429 and 535 nm. This spectrum has properties similar to that of both $[(TMpyP)Co^{I}]^{3+}$ (431 and 550 nm) and $[(TMpyP)Co^{II}(O_2^-)]^{3+}$ (426 and 533 nm).

The spectroelectrochemical data in Figure 9 suggest the formation of at least one high oxidation state cobalt porphyrin complex during controlled potential reduction of $[(TMpyP)Co^{II}]^{4+}$ in solutions containing O_2 and benzoic anhydride. These results are consistent with the electrochemical data presented earlier and suggest the overall sequence of steps given in Scheme II where the benzoic anhydride products could be either a free peroxybenzoate anion or a peroxybenzoate radical.

The initial formation of $[(TMpyP)Co^{II}(O_2^-)]^{3+}$ and the high oxidation state cobalt porphyrin product which is formed in the presence of benzoic anhydride was independently investigated by spectroscopically monitoring the homogeneous reactions between superoxide ion and $[(TMpyP)Co^{II}]^{4+}$ in the presence and absence of benzoic anhydride. The product obtained upon addition of O_2^- to $[(TMpyP)Co^{II}]^{4+}$ in DMF solutions without benzoic anhydride gives the spectrum shown in Figure 10. This spectrum is similar to the one obtained by thin-layer electroreduction of

Scheme III

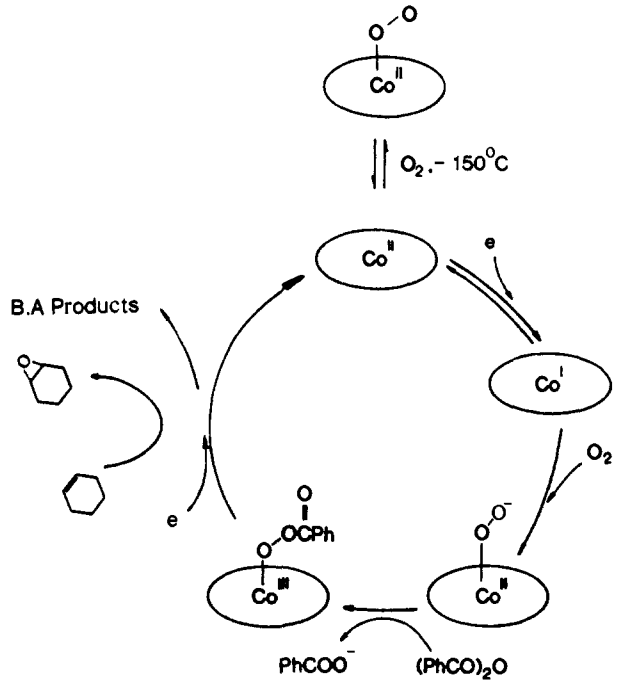

$[(TMpyP)Co^{II}]^{4+}$ under O_2 (see Figure 8b) and is assigned as the superoxide complex, $[(TMpyP)Co^{II}(O_2^-)]^{3+}$.

The spectrum of the product formed after addition of both benzoic anhydride and O_2^- to $[(TMpyP)Co^{II}]^{4+}$ in DMF is shown by the solid line in Figure 10. This spectrum has bands at 459 and 566 nm and is similar to the spectrum obtained between 50 and 175 s during the controlled potential thin-layer electroreduction of $[(TMpyP)Co^{II}]^{4+}$ under O_2 in the presence of benzoic anhydride (see Figure 9). This spectrum has UV–visible characteristics resembling monomeric cobalt(III) porphyrins and is assigned as $[(TMpyP)Co^{III}(O_2COPh)]^{4+}$.

The pathway in which the initial $[(TMpyP)Co^{II}]^{4+}$ complex is regenerated from the high oxidation state cobalt derivative is unknown. However, it has been demonstrated that high-valent oxo complexes of Mn,[16,17,38,39] Fe,[39,40] and Cr[39,41] porphyrins can act as catalysts in the epoxidations of alkenes, and similar epoxidations also occur during the controlled potential reduction of $[(TMpyP)Co^{II}]^{4+}$ in DMF containing O_2, benzoic anhydride, and cyclohexene. These results could suggest the formation of a transient Co(IV)–oxo complex and are described below.

A DMF solution containing 0.36 mM $[(TMpyP)Co^{II}]^{4+}$, 150 mM cyclohexene, 0.4 M benzoic anhydride, and 0.2 M TBAP was electrolyzed at −0.58 V under a continuous stream of O_2. As the electrolysis progressed, samples of this solution were injected into the gas chromatograph (GC). The area of the peak corresponding to cyclohexene oxide increased linearly with time of electrolysis until 4.5 h, after which, it remained constant. After 4.5 h of electrolysis, the concentration of cyclohexene oxide was equal to 20 mM based on measurements of solutions containing authentic cyclohexene oxide. Controlled potential electrolysis of a DMF solution containing 150 mM cyclohexene, 0.4 M benzoic anhydride, and 0.2 M TBAP without the porphyrin led to only small amounts (4 mM) of cyclohexene oxide.

Both $[(TMpyP)Co^{II}]^{4+}$ and benzoic anhydride are needed for the catalytic epoxidation of cyclohexene. An analysis of the GC data for cyclohexene oxide gives a value of 55 turnovers for the $[(TMpyP)Co^{II}]^{4+}$ catalyst during 4.5 h. This corresponds to a Faradaic efficiency of about 45.5% during this period. The efficiency of this electrocatalytic epoxidation is about 5 times higher than the minimum of 11 turnovers in 6 h reported for electroreduced (TPP)MnCl in the presence of 1-methylimidazole and cyclooctene in CH_2Cl_2 containing O_2.[16]

All of the data is self-consistent and fits the overall mechanism shown in Scheme III for the catalytic reduction of O_2 by $[(TMpyP)Co^{II}]^{4+}$ in the presence of benzoic anhydride and cyclohexene.

In summary, this paper presents the first example for the binding of O_2 by a Co(I) porphyrin as well as the first use of a Co(I) porphyrin for the electrocatalytic reduction of O_2 under any solution conditions. In addition, the formation of a high oxidation state cobalt complex during controlled potential reduction of the cobalt(II) derivative is also reported for the first time in porphyrin chemistry. The catalytically active species may be a Co(IV)–oxo complex,[42] but other reactive species might also be generated in the overall catalytic reduction of O_2.[44]

Thin-layer UV–visible spectroelectrochemistry proved to be essential for characterizing the types of species formed during the catalytic reduction of O_2 and $[(TMpyP)Co^{II}]^{4+}$, and this combined electrochemical–spectroscopic technique should be useful in further studies involving the catalytic reaction of O_2 by other electrogenerated metalloporphyrins having low-valent central metals. These studies are now in progress.

Acknowledgment. The support of the National Institutes of Health (Grant GM-25172) and the National Science Foundation (Grant INT-8413696) is gratefully acknowledged.

(38) (a) Groves, J. T.; Watanabe, Y.; McMurry, T. J. *J. Am. Chem. Soc.* **1983**, *105*, 4489. (b) Smegal, J. A.; Hill, C. L. *J. Am. Chem. Soc.* **1983**, *105*, 3515.

(39) Traylor, T. G.; Miksztal, A. R. *J. Am. Chem. Soc.* **1989**, *111*, 7443.

(40) (a) Groves, J. T.; Neumann, R. *J. Am. Chem. Soc.* **1987**, *109*, 5045. (b) Breslow, R.; Brown, A. B.; McCullough, R. D.; White, P. W. *J. Am. Chem. Soc.* **1989**, *111*, 4517.

(41) Garrison, J. M.; Osiovic, D.; Bruice, T. C. *J. Am. Chem. Soc.* **1989**, *111*, 4960.

(42) Peroxybenzoate anions or peroxybenzoate radicals may also be chemical oxidants for the selective conversion of olefins to epoxides. In addition, a Co(III) porphyrin cation radical complex has been suggested as an intermediate in the epoxidation of olefins by using (TTP)Co as the catalyst.[43] However, the formation of this type of species is ruled out in the present study by the fact that UV–visible spectral data give no evidence of cobalt porphyrin cation radicals in the catalytic cycle (see Figures 9 and 10).

(43) Haber, J.; Mlodnicka, T.; Witko, M. *J. Mol. Catal.* **1989**, *52*, 85.

(44) The catalytic regeneration of $(TMpyP)Co^{II}$ might also proceed via two high oxidation state complexes rather than only one. For example, $[(TMpyP)Co^{III}(O_2COPh)]^{4+}$ could be converted to $(TMpyP)Co^{IV}{=}O$ by a homogeneous cleavage of the peroxy O–O bond. A transient Co(IV)–oxo species has been postulated to occur during the catalytic oxidation of olefins by $(Ia)Co^{II}$ where the ligand Ia = the bis-salicylamide dianion 2,3-bis(3,5-dichloro-2-oxybenzamido)-2,3-dimethylbutane in the presence of *tert*-butyl hydroperoxide and iodosylbenzene.[45] Spectroelectrochemical data in this present study might also support this type of mechanism.

(45) Koola, J. D.; Kochi, J. K. *J. Org. Chem.* **1987**, *52*, 4545.